

# THE TEMPERATURE DEPENDENCE OF THE EFFECTIVE REFRACTIVE INDEX OF $TE_1$ AND $TM_1$ MODES IN OPTICAL SOL–GEL WAVEGUIDES OVER A WIDE TEMPERATURE RANGE

N. E. Nikolaev, S. V. Pavlov, N. S. Trofimov, and T. K. Chekhlova\*

*Peoples' Friendship University of Russia  
Miklukho Maklay Str., 6, Moscow 117198, Russia*

\*Corresponding author e-mail: tchekhlova@mail.ru

## Abstract

We obtain the temperature dependences of the effective refractive index on the parameters of the sol–gel film. We found and explain the differences in the temperature characteristics of the sol–gel waveguides for the transverse electric (TE) and transverse magnetic (TM) modes. We consider the features of these dependencies and make physical interpretations of them under high-temperature conditions.

**Keywords:** integrated optics, optical waveguide, effective refractive index, sol–gel method, optical temperature coefficient.

## 1. Introduction

Further development of telecommunication systems requires usage of new technologies and materials. They provide improved characteristics for the basic elements of these systems, such as optical waveguides, splitters, switches, and others based on thin films fabricated of different materials.

In recent years, the attention of the researchers is attracted to waveguides based on the films manufactured by the sol–gel method. This technology is simple enough, economical, and provides good optical characteristics of the waveguides. Moreover, sol–gel films possess a number of interesting properties, among which are the possibility of varying the refractive index in wide limits by changing the fabrication-process parameters, i.e., high photosensitivity, possibility to doping with different elements, etc. [1–4].

One of the most interesting properties of sol–gel films is a large negative optical temperature coefficient (OTC), which allows using them in waveguide devices with thermocontrol such as directional splitters, switches, and commutators [5].

Manufacturing of the integrated optics devices based on the sol–gel-film technology generates a need for more detailed research of temperature properties of the optical waveguides fabricated of these materials.

Studies of the temperature dependence of the effective refractive index (ERI) made in [6] discovered the difference in the form of the dependences for the TE and TM waveguide modes in the temperature range from 0 to 100°C. It was shown in [7] that the observed features are caused by two competitive factors — the temperature dependence of the film thickness (positive factor) and the temperature dependence of the refractive index of the film material (negative factor, since the film material has negative OTC).

Our aim in this work is to make clear how these two indicated factors influence the behavior of the temperature dependences of optical waveguides based on TiO<sub>2</sub>–SiO<sub>2</sub> sol–gel films in a wide temperature range for different TE and TM waveguide modes.

## 2. Temperature Dependence of the Effective Refractive Index

The effective refractive index of the waveguide modes is calculated using the dispersion equations, which determine the relations between the corresponding mode ERI, the thickness of the waveguide layer, the wavelength, and the refractive indices of the media forming the waveguide with taking into account their temperature dependences.

The dispersion equations are as follows:

$$\frac{2\pi}{\lambda} h(T) \sqrt{n_2(T)^2 - n_{\text{eff}}^2} = \arctan \left[ \frac{\sqrt{n_{\text{eff}}^2 - n_1^2}}{\sqrt{n_2(T)^2 - n_{\text{eff}}^2}} \right] + \arctan \left[ \frac{\sqrt{n_{\text{eff}}^2 - n_3(T)^2}}{\sqrt{n_2(T)^2 - n_{\text{eff}}^2}} \right] + \pi(m - 1) \quad (1)$$

for the TE modes, and

$$\frac{2\pi}{\lambda} h(T) \sqrt{n_2(T)^2 - n_{\text{eff}}^2} = \arctan \left[ \frac{n_2^2 \sqrt{n_{\text{eff}}^2 - n_1^2}}{n_1^2 \sqrt{n_2(T)^2 - n_{\text{eff}}^2}} \right] + \arctan \left[ \frac{n_2^2 \sqrt{n_{\text{eff}}^2 - n_3(T)^2}}{n_3^2 \sqrt{n_2(T)^2 - n_{\text{eff}}^2}} \right] + \pi(m - 1) \quad (2)$$

for the TM modes, where  $\lambda$  is the wavelength of the radiation source,  $n_{\text{eff}}$  is the ERI of the waveguide mode,  $n_1$ ,  $n_2$ , are  $n_3$  are the refractive indices of air, film, and substrate, respectively, and  $m$  is the coefficient of the waveguide wave (mode).

The temperature dependences of the refractive index and the thickness of TiO<sub>2</sub>–SiO<sub>2</sub> sol–gel films were calculated using functions  $n_2(T)$  and  $h(T)$  obtained experimentally and approximated by the following polynomials:

$$n_2(T) = -2.047 \cdot 10^{-7} T^2 - 2.185 \cdot 10^{-5} T + n_2, \quad h(T) = (1.168 \cdot 10^{-6} T^2 - 1.838 \cdot 10^{-5} T + 1)h.$$

The behavior of these characteristics for the TE<sub>1</sub> and TM<sub>1</sub> waveguide modes at temperatures near 100°C [6] suggests that some new features can show up on the further temperature increase. Encouraged by this assumption, we investigated the characteristics of the optical waveguides fabricated from TiO<sub>2</sub>–SiO<sub>2</sub> sol–gel films. These studies were carried out in a wide temperature range from 0 to 400°C. The ERI emperature dependences were calculated for the waveguides with the refractive index 1.8, because the studied features of the characteristics are much more expressed at high refractive index.

The ERI emperature dependences for the TE<sub>1</sub> and TM<sub>1</sub> waveguide modes were calculated for the film thickness  $h$  lying in the range from 0.14 to 0.5  $\mu\text{m}$ . In these calculations, the film refractive index  $n_2$  has values 1.49, 1.55, and 1.8.

The analysis of the obtained results for refractive indices 1.48 and 1.55 shows that, for the film thickness within the stated range, the ERI( $T$ )-function evolution for the TE<sub>1</sub> and TM<sub>1</sub> waveguide modes is the same for the both modes, i.e., the ERI values monotonically decrease with the temperature increase, and the curves for these modes are convex. So, the waveguides have negative temperature coefficient, and the behavior of the dependence ERI( $T$ ) is conditioned by the negative OTC of the film material. A typical function ERI( $T$ ) corresponding to  $h = 0.5 \mu\text{m}$  and  $n_2 = 1.55$  is presented in Fig. 1.

We observed interesting dependences of ERI( $T$ ) for the refractive index  $n_2 = 1.8$ . The behavior of the dependence of ERI( $T$ ) differs sufficiently for thick (from 0.34 up to 0.5  $\mu\text{m}$ ) and thin (from 0.14 to 0.34  $\mu\text{m}$ ) films. For thick films, the behavior of the function ERI( $T$ ) (Fig. 2) is similar to the function shown in Fig. 1. As the film thickness increases, the behavior of this function coincides with the behavior of the function corresponding to  $n_2 = 1.55$ , i.e., the curves corresponding to the TE<sub>1</sub> and TM<sub>1</sub> modes are convex, and the degree of convexity increases with the film thickness (Figs. 2 a and b).

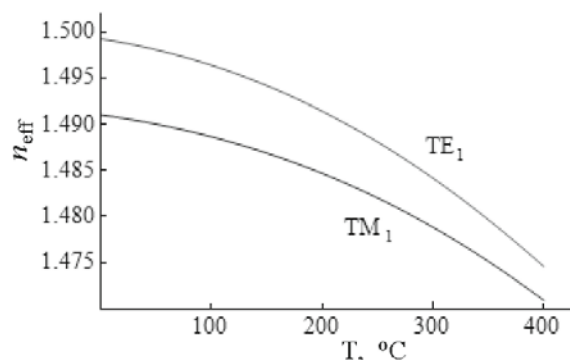


**Fig. 1.** The ERI temperature dependences for the TE<sub>1</sub> and TM<sub>1</sub> modes at  $n_2 = 1.55$  and  $h = 0.5 \mu\text{m}$ .

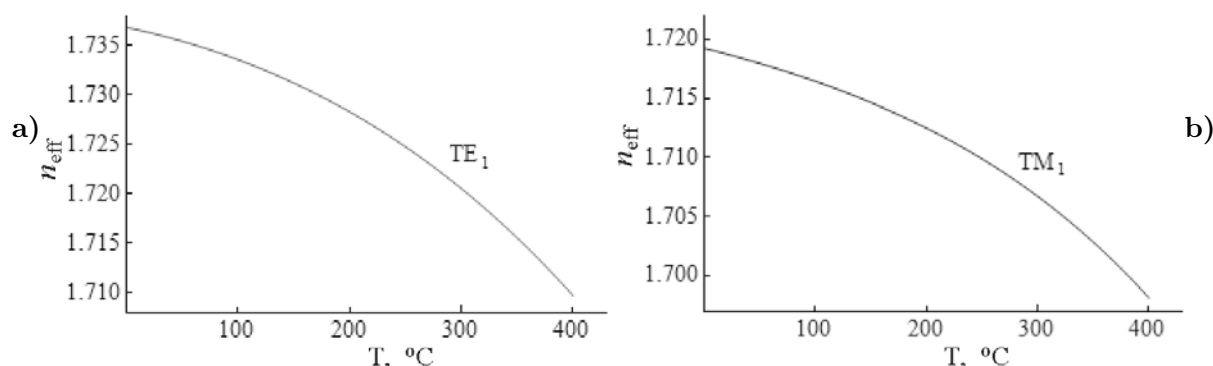


**Fig. 2.** The ERI temperature dependences for the TE<sub>1</sub> (a) and TM<sub>1</sub> (b) modes at  $n_2 = 1.8$  and  $h = 0.5 \mu\text{m}$ .

However, the behavior of this function drastically changes for films with small thickness (equal to or less than 0.34  $\mu\text{m}$ ), and the behavior of the curves corresponding to the TE<sub>1</sub> and TM<sub>1</sub> modes become substantially different. For example, for a film thickness of 0.34  $\mu\text{m}$ , the function ERI( $T$ ) corresponding to the TE<sub>1</sub> mode is a convex curve (as in the previous cases), and the function ERI( $T$ ) corresponding to the TM<sub>1</sub> mode is a concave curve.

The changing of the dependence ERI( $T$ ) for the TE<sub>1</sub> mode with the variation of the film thickness (from 0.14 to 0.30  $\mu\text{m}$ ) is shown on Fig. 3.

At the film thickness of 0.14  $\mu\text{m}$  and the temperature range from 0 to 80°C, the curve is concave and has a minimum at 80°C. With temperature increase the ERI also increases, so the ERI temperature coefficient (ERI TC) in this range is positive (Fig. 3 a). The negative ERI TC (shown by the curve decline) in the temperature range 0–80°C has the value of  $0.7 \cdot 10^{-5}$ , and the positive ERI TC (increase of the curve) in the temperature range from 80 to 400°C is  $1.2 \cdot 10^{-5}$ .

As the film thickness increases up to 0.165  $\mu\text{m}$ , the curve has the second extremum at a temperature

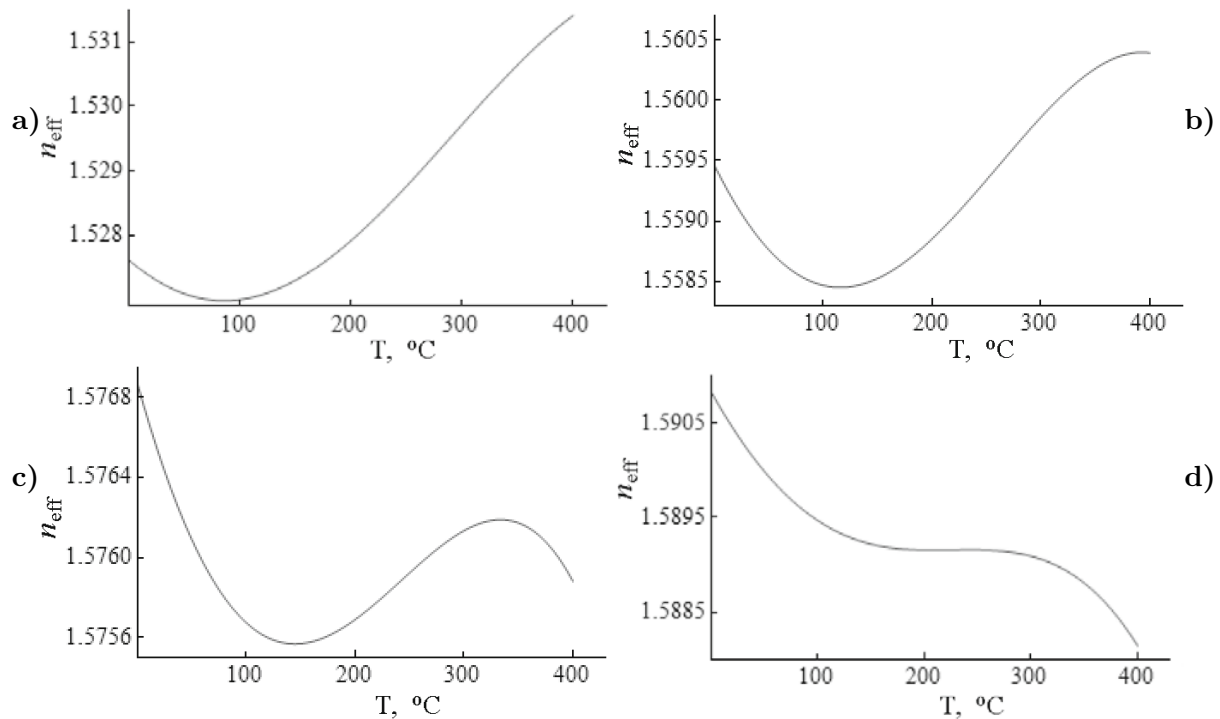


**Fig. 3.** The ERI temperature dependences for the  $TE_1$  mode at  $n_2 = 1.8$  and  $h = 0.140$  (a),  $0.165$  (b),  $0.180$  (c), and  $0.193 \mu\text{m}$  (d).

near  $400^\circ\text{C}$  (Fig. 3 b). At higher temperatures, the TC becomes negative again. As this fact takes place, the position of the first extremum moves towards higher temperature ( $120^\circ\text{C}$ ), and the ERI TCs have the same absolute values  $1 \cdot 10^{-5}$ .

With further-film thickness increase, the extrema moves towards each other (Fig. 3 c), i.e., the low-temperature extremum moves to the right, and the high-temperature extremum moves to the left. So, it results in a decrease in the difference of the extremum values. At a film thickness of  $0.180 \mu\text{m}$ , the negative ERI TC increases in the temperature range from  $0$  to  $140^\circ\text{C}$  up to  $-1.2 \cdot 10^{-5}$ , and the positive ERI TC in the temperature range from  $140$  to  $400^\circ\text{C}$  decreases to  $0.3 \cdot 10^{-5}$ .

At a film thickness of  $0.193 \mu\text{m}$ , we observe that the curve has a horizontal segment in the temperature range approximately from  $180$  to  $260^\circ\text{C}$ , with the ERI value equal to  $1.593$ . Within this segment, the action of both temperature factors (positive and negative) is compensated, and the ERI does not depend on temperature (Fig. 3 d).

Further increase in the film thickness ( $0.20 \mu\text{m}$ ) causes the change of the curve shaper — a concave curve in the temperature range  $0$ – $200^\circ\text{C}$  and a convex curve in the temperature range  $200$ – $400^\circ\text{C}$ . An inflection point of the curve is located at  $200^\circ\text{C}$ . When the film thickness increases up to  $0.30 \mu\text{m}$  and higher, the curve becomes uniformly convex. The values of the ERI TC are  $-3 \cdot 10^{-5}$  in the temperature range from  $0$  to  $200^\circ\text{C}$ , and  $-10 \cdot 10^{-5}$  in the temperature range from  $250$  to  $400^\circ\text{C}$ .

For the  $TM_1$  mode, the function  $ERI(T)$  for thin films ( $0.140$ – $0.20 \mu\text{m}$ ) also has extremum, however, it is shifted to low temperatures with respect to the  $TE_1$  mode, and the change location from  $8$  to  $41^\circ\text{C}$  with the film thickness increase within the stated limits. Our studies showed that the  $ERI(T)$  function behavior for the  $TM_1$  mode is similar to that for the  $TE_1$  mode, but all the characteristic points are

shifted towards lower film thicknesses (Fig. 4).

Experimental studies of the temperature characteristics of sol-gel waveguides showed that for the most part of studied samples the temperature coefficient of the ERI was negative. However, for the  $TM_1$  mode, at a film thickness of  $0.2342 \mu\text{m}$ , the positive ERI TC was observed in the temperature range from 20 to  $50^\circ\text{C}$ , which corresponds to the results of our calculations.

### 3. Results and Discussion

Our studies proved the assumptions made in [7] that the dependence  $ERI(T)$  is determined by two competitive factors — the temperature dependence of the film thickness (positive factor), and the temperature dependence of the refractive index of the film material (negative factor, since the film material has the negative OTC). In addition, the action of the negative factor increases with increase in the film thickness, since the thickness increase results in the concentration of the wave field growth, as shown in [6].

Lowering of the ERI values at higher temperatures and the convex shape of the curves (see Figs. 1 and 2) reflect the dominance of the negative OTC of the film material. This conclusion follows from the estimated contribution of the factors stated, presented in [7] where the temperature dependence  $ERI(T)$  was calculated for two different alterations: (1) consideration of the negative-film-material OTC assuming the film thickness being temperature-independent and (2) consideration of the film thickness variations caused by the temperature change at a fixed film refractive index.

For the thin films (see Fig. 3), the film-thickness temperature-dependence factor grows up and its contribution to the ERI is positive. In this case, the influence of the film-material negative OTC is small, due to low wave-field concentration in the film, as shown in [6].

The extremum points of the ERI curve correspond to equal contributions of the two factors considered. A subsequent increase in the function  $ERI(T)$  is caused by a greater influence of the positive factor (increase in the film thickness with temperature) on the ERI, which increases the ERI value. As the temperature overgrows the first extremum point, the increase in the ERI value at first becomes slower, since the competitive negative factor increases with the film-thickness increase, then the action of both factors becomes equal (the second extremum), and after that the curve  $ERI(T)$  becomes convex and decreases, showing a dominance of the negative factor.

The aforesaid is true for both considered modes. However, for the  $TM_1$  mode, the features of the ERI temperature dependence (occurrence of the extrema and their behavior with the varying thickness) show themselves at higher values of the film thickness. This occurs due to the smaller concentration of the waveguide mode field in sol-gel films, and the action of a negative factor decreases in accordance with the portion of the mode power propagating in the sol-gel film.

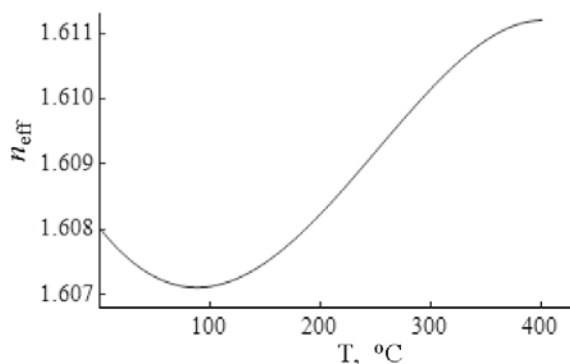


**Fig. 4.** The ERI temperature dependences for the  $TM_1$  mode at  $n_2 = 1.8$  and  $h = 0.283 \mu\text{m}$ .

### References

1. M. A. Fardad, O. Mishechkin, and M. Fallahi, *J. Lightwave Technol.*, **19**, 84 (2001).
2. S. Saini, R. Kurrat, J. E. Prenosil, and J. J. Ramsden, *J. Phys. D: Appl. Phys.*, **27**, 1134 (1994).

3. Y. Enami, M. Kawazu, A. K.-Y. Jen, et al., *J. Lightwave Technol.*, **21**, 2053 (1994).
4. Y. Beregovski, A. Fardad, H. Luo, and M. Fallahi, *Opt. Commun.*, **164**, 57 (1999).
5. X. Wang, L. Xu, D. Li, et al., *J. Appl. Phys.*, **94**, 4228 (2003).
6. N. E. Nikolaev, S. V. Pavlov, N. S. Trofimov, and T. K. Chekhlova, *J. Commun. Technol. Electron.*, **57**, 15 (2012).
7. T. K. Chekhlova, S. V. Zhivtsov, and E. I. Grabovskii, *J. Commun. Technol. Electron.*, **51**, 804 (2006).